Atom laser based on four-wave mixing with Bose-Einstein condensates in nonlinear lattices

T. Wasak,[1,*] V. V. Konotop,[2] and M. Trippenbach[1]

[1]*Faculty of Physics, University of Warsaw, ul. Hoża 69, PL-00-681 Warszawa, Poland*

[2]*Centro de Física Teórica e Computacional and Departamento de Física, Faculdade de Ciências, Universidade de Lisboa, Avenida Professor Gama Pinto 2, 1649-003 Lisboa, Portugal*

(Received 29 July 2013; published 13 December 2013)

Optical lattices are typically used to modify the dispersion relation of the matter wave, in particular, to ensure resonant conditions for multiwave interactions. Here we propose an alternative mechanism of wave interactions. It can be implemented using a nonlinear lattice and modifies the momentum conservation law of the interacting atoms, leaving the energy conservation unchanged. We propose to apply this phenomenon to construct an atom laser via a resonant four-wave mixing process.

DOI: 10.1103/PhysRevA.88.063626 PACS number(s): 67.85.−d, 03.75.Be, 42.65.Hw

Resonant interactions in a nonlinear system occur when matching conditions, ensuring energy and momentum conservation, are satisfied for the modes coupled by the nonlinearity. This fundamental phenomenon has been studied especially well in the context of optical applications [1] and spectroscopy [2]. More than a decade ago it was also applied to the dynamics of atomic Bose-Einstein condensates (BECs) [3], where four-wave mixing (FWM) was demonstrated experimentally [4], and became an important contribution to the field of nonlinear atom optics [5]. The physics of matter-wave implementation of the FWM is based on binary collisions in ultracold atomic gases. Due to the two-body interactions, two matter waves form a grating from which a third wave diffracts, thus generating a fourth wave. This process has been used for coherent matter-wave amplification [6] and generation of correlated atom pairs [7–11].

A very important application of nonlinear ultracold atoms systems is the atom laser [12], i.e., a source of coherent matter waves. It opened the way to fascinating applications of atom optics [5] and interferometry [13]. In this article we propose yet another realization of the atom laser, which is based on the FWM process in a nonlinear lattice.

Due to the constraints imposed by the conservation laws, mode interactions are very sensitive to the dimensionality of the system. In particular, the conservation laws require the magnitudes of all atomic momenta in the center-of-mass frame to be equal. For atoms in a single internal state, it requires at least a two-dimensional (2D) geometry [3] and is completely inhibited in the 1D setting. In order to make the phenomenon observable in one dimension, one has to employ additional physical tools. In nonlinear optics it has been realized that artificial dispersion, introduced, for instance, by periodic variation of medium parameters, can completely change the propagation and allow for resonant mode interactions in 1D systems. Among relevant studies in this direction we mention resonant mode interactions in 1D nonlinear photonic crystals [1], in nonlinear discrete systems [14], and, more recently, in quasi-1D BECs loaded in (linear) optical lattices. This phenomenon has been studied both theoretically [15] and experimentally [8,16].

The main physical ingredient introduced by the *linear* lattice is a change of the dispersion relation or, in terms of the BEC application, of the energy dependence on the Bloch vector (quasimomentum) of the macroscopic wave function. Thus, considering the matching conditions, the linear optical lattice modifies the energy conservation law $E(k_1) + E(k_2) = E(k_3) + E(k_4)$ [where $E(k)$ is now a periodic rather than a parabolic function], not affecting the momentum conservation. It is thus natural to explore the implementation of an alternative realization of resonant mode interactions, namely, the possibility of *modification of the momentum conservation not affecting the conservation of the energy*.

In order to address this possibility we recall that wave mixing is an essentially nonlinear phenomenon allowing for modification of matching conditions by means of modulations of the nonlinearity. In this context we note that in nonlinear optics the multimode processes in combined linear and nonlinear lattices (nonlinear photonic crystals) have already received considerable attention, triggered by Ref. [17]. In BECs, where the nonlinearity stems from the two-body interactions, a *nonlinear* spatial lattice can be induced by periodic modulation of the scattering lengths using the Feshbach resonance. Such a pure nonlinear lattice has recently been implemented experimentally [18] and was shown to be a useful tool for managing superfluid and Josephson currents [19] or soliton dynamics [20]. The main goal of this paper is to propose a mechanism for a coherent matter wave formation in a nonlinear lattice.

In the mean-field approximation a 3D BEC loaded in a nonlinear optical lattice $G(x)$ is described by the Gross-Pitaevskii equation (GPE) for the order parameter Ψ,

$$i\hbar\frac{\partial\Psi}{\partial t} = -\frac{\hbar^2}{2m}\nabla^2\Psi + G(x)|\Psi|^2\Psi + \frac{m}{2}\left(\omega_y^2 y^2 + \omega_z^2 z^2\right)\Psi, \tag{1}$$

where $\omega_{y,z}$ are frequencies of the harmonic trap in the transverse direction and the nonlinear coefficient $G(x)$ describes the spatial modulation of the scattering length. The particular shape of the nonlinear lattice is not crucial: here we choose $G(x) = g[1 + \alpha\cos(\kappa x)]$, where $g = 4\pi\hbar^2 a_s/m$, a_s is the spatially averaged value of the scattering length, m is the atomic mass, $\kappa = 2\pi/d$ is the lattice vector, d is the lattice period, and α is the lattice depth. We consider an

*tomasz.wasak@fuw.edu.pl

elongated BEC along the x axis, which is also the direction of the Bragg pulses imposing momentum on the condensate. We assume that in the perpendicular direction there is strong confinement, hence the evolution will be quasi-1D. Consequently we develop a 1D phase-matching analysis (although we emphasize that our numerical simulations below are fully 3D).

Considering an FWM involving a source wave packet (mother cloud) with momentum $\hbar k_0$ and wave packets with momenta $\hbar k_1$, and $\hbar k_2$ (daughter clouds), conservation of the energy requires

$$2k_0^2 = k_1^2 + k_2^2. \tag{2}$$

For a homogeneous condensate, mother and daughters do not interact resonantly because energy conservation and momentum conservation cannot be (nontrivially) simultaneously satisfied. If, however, at some instant the nonlinear lattice is switched on, wave mixing becomes possible. Indeed, the wave vectors entering the problem and the lattice period satisfy the modified momentum conservation law, given by

$$2k_0 = k_1 + k_2 \pm \kappa. \tag{3}$$

The relation among the involved parameters is illustrated schematically in Figs. 1(a) and 1(b). For fixed κ one can identify the resonant FWM wave vectors in the following way. Choose the initial k_0 and draw a vertical dotted line [see Fig. 1(a)]. The wave numbers of the daughter wave packets (k_1 and k_2) are given by the abscissa of the crossing points of the vertical dotted line with the lighter (red) solid curve.

One can readily establish that for a given nonlinear lattice κ, there exists a threshold $|k_0| = |\kappa|/4$ [see Fig. 1(a)], below which FWM does not occur. Above this value the mother cloud generates two daughter clouds, which move in opposite directions [central (blue) shaded region] or the same direction [left (red) and right (gray) shaded regions). The respective geometry of the wave vectors involved become particularly evident in the plane (k_1,k_2) as shown in Fig. 1(b). Indeed the momenta of the generated wave packets at the given k_0 and κ are determined by the intersection of the circle of radius $\sqrt{2}|k_0|$ [as follows from Eq. (2)] and the line given by Eq. (3). While the position of the circle is fixed by its center located at the origin, the position of the line varies depending on the relation between k_0 and κ. Let k_0 be fixed and the lattice parameter κ be varying. Then the FWM process is possible (the line crosses the circle) if $0 < \kappa < 4|k_0|$ [the circle between the two solid lines in Fig. 1(b)]. In a more narrow region, $(2-\sqrt{2})|k_0| < \kappa < (2+\sqrt{2})|k_0|$, the produced wave packets propagate in opposite directions [any line between two dashed lines in Fig. 1(b) will cross the circle in the second and fourth quadrants]. If, however, $0 < \kappa < (2-\sqrt{2})|k_0|$ or $(2+\sqrt{2})|k_0| < \kappa < 4k_0$), then the generated wave packets will propagate in the same direction.

In the current study we concentrate on the degenerate case, where one of the final momenta is exactly the same as the initial one, i.e., in the case $k_0 = k_2 = -k_1 = \kappa/2$ [shown in Fig. 1(a)] (the general case is described elsewhere [21]). As a reference physical system we have chosen the ^{174}Yb BEC used in the original experiment [18], where spatial modulation of the scattering length up to 250 nm on a scale of 278 nm

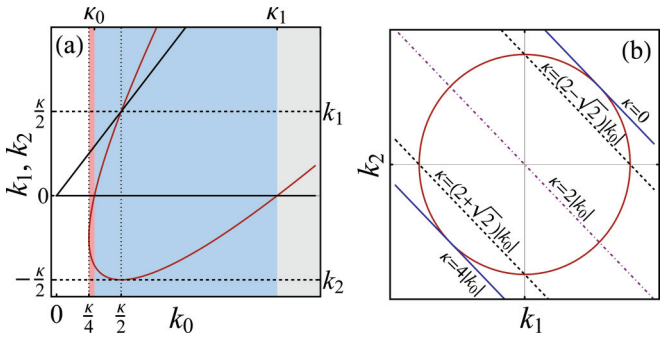

FIG. 1. (Color online) (a) Schematic of the FWM wave vectors involved in the wave mixing process for the fixed nonlinear lattice wave vector κ. The branches of the solutions $k_{1,2}$ for a given $k_0 \geqslant 0$ satisfy the momentum conservation law with a plus sign in (3) [the case $k_0 \leqslant 0$, corresponding to a minus "−" sign in (3), is considered similarly]. Vertical dotted and horizontal dashed lines show an example of the daughter pulse wave vectors k_1 and k_2, whose values are obtained from the intersection with the vertical axis; data are chosen to correspond to the numerical experiment shown in Fig. 2: this is the degenerated case $k_1 = -k_2 = k_0 = \kappa/2$. The solid black line with the slope indicates $k_1 = k_0$ (or, alternatively, $k_2 = k_0$). (b) Geometry of the wave vectors involved in the FWM process at different lattice vectors. The diagonal dot-dashed line passing through the center corresponds to the degenerated case. The region of parameter k_0 for which FWM occurs can be divided into three subdomains (shaded red, blue, and gray, from left to right). The narrow left (red) shaded region ($\frac{|\kappa|}{4} \leqslant |k_0| \leqslant \frac{|\kappa|}{2+\sqrt{2}} \equiv \kappa_0$) shows the configuration for which daughter waves propagate in the same direction, which is opposite to the direction of the source wave; the central (blue) shaded region ($\kappa_0 \leqslant |k_0| \leqslant \frac{|\kappa|}{2-\sqrt{2}} \equiv \kappa_1$), daughter waves propagate in opposite directions; and the right (gray) shaded region ($\kappa_1 \leqslant |k_0|$), daughter waves propagate in the same direction as the source wave.

was observed. We performed full 3D numerical simulations using the GPE. We used the atomic mass of ytterbium $m = 2.89 \times 10^{-25}$ kg and the background scattering length $a = 5.55$ nm. We started by preparing a system of $N = 10^4$ atoms in the ground state of an anisotropic harmonic trap with axial frequency $\omega_x = 2\pi \times 32\ \mathrm{s}^{-1}$ and radial frequencies $\omega_y = 2\pi \times 1210\ \mathrm{s}^{-1}$ and $\omega_z = 2\pi \times 1990\ \mathrm{s}^{-1}$. Note that the axial frequency is the same as used in the experiment, but the radial frequencies are 10 times larger, and the number of atoms is 10 times smaller, compared to the data reported in Ref. [18]. Consequently the density of the atomic cloud in the simulation was lower than the experimental value.

Using the ground state described above we start the actual FWM process. We simultaneously turn on the nonlinear lattice with lattice vector $\kappa = 10.15 a_{\mathrm{ho,x}}^{-1}$ ($a_{\mathrm{ho,x}} = \sqrt{\hbar/m\omega_x}$ and $d = 0.834\ \mu$m) and amplitude $\alpha = 0.4$ and impose a pair of Bragg pulses, to increase its mean BEC velocity up to $\hbar k_0/m = 1.375$ mm/s, corresponding to $k_0 = \kappa/2$. Two other actions were taken to increase the desired effect. We turn off the trap in the x direction and reduce the coupling constant g by a factor of 10^2. The latter decreases the spreading of the momentum distribution and can be done by means of Feshbach resonance.

We emphasize that in the arrangement described above the mean kinetic energy of the BEC wave packet is equal to $E = \hbar^2\kappa^2/8m$, and it is smaller than the energy spacing

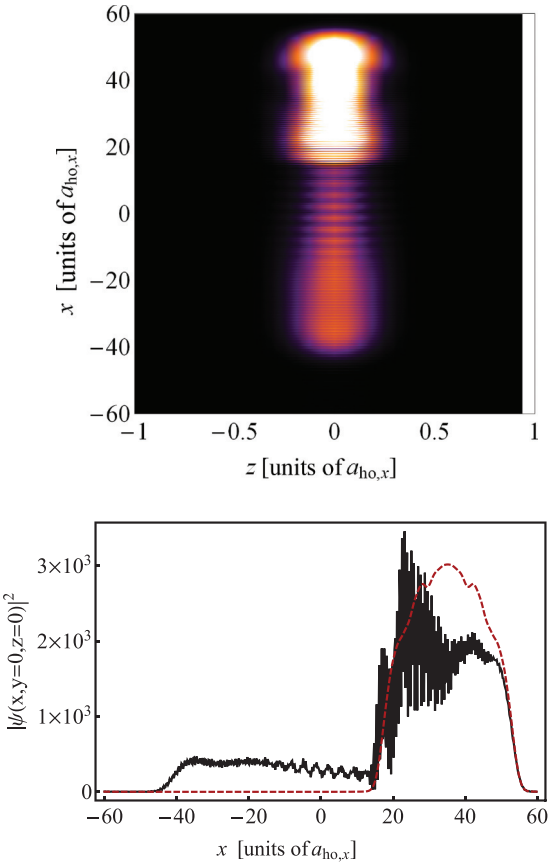

FIG. 2. (Color online) Density of the atomic cloud at $t = 34.45$ ms. Top: x-z cut through the density at $y = 0$. Bottom: Density cut (in units of $a_{\mathrm{ho,x}}^{-3}$) at $y = z = 0$. The mother cloud is moving along the x axis at velocity $k_0 = \kappa/2$ and creates a wave packet with momentum $k_1 = k_0 = -k_2 = \kappa/2$ [indicated in Fig. 1(a)]. For comparison, the dashed (red) line shows the density of the BEC when the nonlinear lattice is absent, $\alpha = 0$.

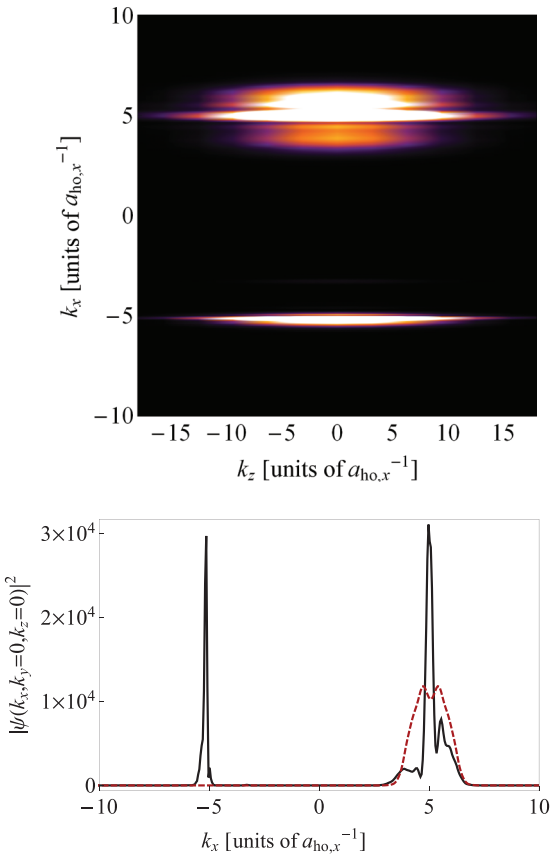

FIG. 3. (Color online) Momentum distribution of the atomic cloud at $t = 34.45$ ms. Top: x-z cut through the momentum distribution of the atomic cloud at $k_y = 0$. Bottom: Momentum distribution cut (in units of $a_{\mathrm{ho,x}}^{3}$) at $k_y = k_z = 0$. Clearly, two distinct peaks are visible in the distribution. The one centered around $k = \kappa/2$ is the mother cloud, consisting of most of the atoms. The second peak is centered around $k = -\kappa/2$. The dashed (red) line shows the distribution of the BEC when the nonlinear lattice is absent, $\alpha = 0$.

between levels of the harmonic trap in the radial direction ($E/\hbar\omega_y = 0.34$ and $E/\hbar\omega_z = 0.21$). This choice prevents the population of the higher excited modes in radial directions. As the confinement in y is weaker than that in z, there is some residual dynamics in this direction, but the movement in z is almost completely frozen.

Our main result is presented in Figs. 2 and 3. In Fig. 2 we show the atom density at $t = 34.45$ ms. Besides the mother wave packet, moving with momentum $k_0 = \kappa/2$, we can distinguish the daughter wave packet as a wave propagating with opposite momentum $k_0 = -\kappa/2$. The top plot shows the x-z cut through the density at $y = 0$. The bottom plot presents the density cut at $y = z = 0$. The visible oscillations in the density result from the overlap of wave packets moving with different wave vectors. To provide more evidence that the daughter wave packet is created with the right momentum, we also include Fig. 3, which shows the momentum distribution. Again, the top plot shows the x-z cut through the momentum distribution at $k_y = 0$ and the bottom plot presents the momentum distribution cut at $k_y = k_z = 0$. Two distinct peaks are visible in the distribution: one is centered around $k = \kappa/2$ (mother cloud) and the second around $k = -\kappa/2$ (daughter cloud). The latter is the *atom laser radiation*, which is coherently emitted from the initial wave packet. The distribution of the source is very different from the initial distribution of the BEC, revealing the internal dynamics of the cloud. Note that the width of the newborn peak is very narrow, indicating a high degree of monochromaticity of the atomic beam. For comparison, the dashed (red) lines in Figs. 2 and 3 show the distribution of the BEC when a nonlinear lattice is absent, $\alpha = 0$.

To gain physical insight into the dynamics we consider the case of a dilute gas tightly bounded in the transverse direction. In the weakly nonlinear limit the order parameter in the leading order can be represented in the factorized form, $\Psi \approx \Phi_\perp(y,z)\psi(x,t)$, where

$$\Phi_\perp(y,z) = \frac{1}{\sqrt{2\pi\sigma_y\sigma_z}} \exp\left[-\left(\frac{y^2}{4\sigma_y^2} + \frac{z^2}{4\sigma_z^2}\right)\right] \qquad (4)$$

is the ground state of the 2D linear oscillator. Now the dynamics in the radial directions remains negligible and we reduce the 3D GPE to the 1D equation for $\psi(x,t)$ [22],

$$i\hbar\frac{\partial\psi}{\partial t} = -\frac{\hbar^2}{2m}\frac{\partial^2\psi}{\partial x^2} + g_{1d}[1 + \alpha\cos(\kappa x)]|\psi|^2\psi, \qquad (5)$$

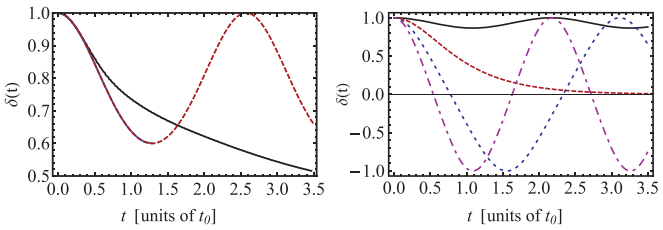

FIG. 4. (Color online) Relative population imbalance $\delta(t)$ of the atomic clouds vs time in units of $t_0 = 2/\omega_x$ for $\alpha = 0.4$. Left: Numerical simulation of the 3D GPE (solid black line); numerical solution of the plane-wave model, (7) [dashed (red) line]; and analytical solution of (8) (solid blue line). Right: Numerical solution of the plane-wave model, (7), for values of $\alpha = 0.25$ (solid black line), $\alpha = 0.5$ [dashed (red) line], $\alpha = 0.75$ [dotted (blue) line], and $\alpha = 1$ [dot-dashed (purple) line]. For $|\alpha| \ll 1$, Eq. (8) gives $\delta(t) = 1 - \alpha^2(\cos(2\gamma t) - 1)$. When $\alpha = 0.5$, $\delta(t) = 1/\cosh(\gamma t)$.

where $g_{1d} = g/4\pi\sigma_y\sigma_z$. Furthermore, to reveal the role of the depth α of the nonlinear lattice we introduce an even simpler model, decomposing the wave function $\Psi(x,t)$ into two wave packets,

$$\psi(x,t) = A_0(t)e^{ik_0x - iE_0t/\hbar} + A_1(t)e^{ik_1x - iE_1t/\hbar}, \tag{6}$$

with $k_0 = -k_1 = \kappa/2$ and $E_0 = E_1 = \hbar^2\kappa^2/8m$. Assuming the amplitudes $A_{0,1}$ to be slowly varying in space we arrive at

$$i\hbar\frac{dA_0}{dt} = g_{1d}n_0A_0 + \frac{g_{1d}\alpha}{2}A_1^*A_0^2 + \frac{g_{1d}\alpha}{2}n_1A_1, \tag{7a}$$

$$i\hbar\frac{dA_1}{dt} = g_{1d}n_1A_1 + \frac{g_{1d}\alpha}{2}A_0^*A_1^2 + \frac{g_{1d}\alpha}{2}n_0A_0. \tag{7b}$$

Here the densities $n_0 = |A_0|^2 + 2|A_1|^2$ and $n_1 = |A_1|^2 + 2|A_0|^2$ are introduced and the asterisk stands for complex conjugation. The above equations preserve the total density, $n = |A_0|^2 + |A_1|^2$, and can be solved by quadratures. We focus on the case where initially $A_1(0) = 0$. Then, defining the relative imbalance of the atoms as $\delta(t) = (|A_0(t)|^2 - |A_1(t)|^2)/n$, we obtain that the evolution is described by the implicit formula

$$\frac{g_{1d}n}{2\hbar}t = \int_\delta^1 \frac{ds}{\sqrt{(1-s^2)(s^2-(1-4\alpha^2))}}. \tag{8}$$

For short times, estimated by $t \lesssim 1/(\gamma\sqrt{1+\alpha^2})$, the population imbalance $\delta(t) = 1 - 2(\alpha\gamma t)^2 + \frac{2}{3}\alpha^2(1+\alpha^2)(\gamma t)^4 + \ldots$, where $\gamma = g_{1d}n/2\hbar$. The dynamics of $\delta(t)$ versus α is illustrated and described in Fig. 4.

To compare the 3D dynamics with the plane-wave model introduced above [Eqs. (7) and (8)], we define $A_i(t) = \sqrt{N_i(t)/L}$, where $L = 2\sqrt{\langle x^2\rangle}$ is the effective length of the condensate and $N_i(t)$ is the total number of atoms in the ith wave. We find that appropriate widths [determining g_{1d} introduced in (5)] are $\sigma_y = \langle y^2\rangle^{1/2} = 0.18a_{\mathrm{ho,x}}$ and $\sigma_z = \langle z^2\rangle^{1/2} = 0.12a_{\mathrm{ho,x}}$. The results of the comparison are shown in Fig. 4(a), where we also include the direct solution, (8). Clearly for short times the agreement between the 3D simulation and the plane-wave model, and even with the analytical solution, (8), is very good. At later times the effects related to spreading of the BEC and the decreasing overlap between mother and daughter wave packets become important, leading to a discrepancy between simulations and the reduced model, (7). Figure 4(b) shows the conversion dynamics for different lattice amplitudes α, as well as the decay of the mother wave packet at the critical value $\alpha = 1/2$.

To summarize, here we have presented the theory of an atom laser, based on the FWM process. Its origin lies in the spatial modulation of the nonlinearity due to two-body interactions between atoms. This modulation affects the momentum conservation, leaving the energy conservation unchanged. We have performed numerical simulations using parameters inspired by experiment [18] and demonstrated a new form of degenerated FWM.

T.W. was funded by the Foundation for Polish Science International Ph.D. Projects Programme cofinanced by the EU European Regional Development Fund, and M.T., by Polish National Science Centre Grant No. DEC-2012/06/M/ST2/00479. V.V.K. was supported by the FCT (Portugal) under Grants No. PTDC/FIS/112624/2009 and No. PEst-OE/FIS/UI0618/2011.

[1] See e.g. G. P. Agrawal, *Nonlinear Fiber Optics* (Academic Press, New York, 1995); A. I. Maimistov and A. M. Basharov, *Nonlinear Optical Waves* (Kluwer Academic, Dordrecht, 1999).
[2] R. W. Boyd, *Nonlinear Optics* (Academic Press, San Diego, CA, 2003).
[3] M. Trippenbach, Y. B. Band, and P. S. Julienne, Opt. Express **3**, 530 (1998); Phys. Rev. A **62**, 023608 (2000).
[4] L. Deng *et al.*, Nature **398**, 218 (1999).
[5] P. Meystre, *Atom Optics* (Springer, New York, 2001), and references therein.
[6] J. M. Vogels, K. Xu, and W. Ketterle, Phys. Rev. Lett. **89**, 020401 (2002); J. M. Vogels, J. K. Chin, and W. Ketterle, *ibid.* **90**, 030403 (2003).
[7] R. G. Dall, L. J. Byron, A. G. Truscott, G. R. Dennis, M. T. Johnsson, and J. J. Hope, Phys. Rev. A **79**, 011601(R) (2009).
[8] D. Pertot, B. Gadway, and D. Schneble, Phys. Rev. Lett. **104**, 200402 (2010).
[9] R. Bücker *et al.*, Nat. Phys. **7**, 608 (2011).
[10] A. Perrin, H. Chang, V. Krachmalnicoff, M. Schellekens, D. Boiron, A. Aspect, and C. I. Westbrook, Phys. Rev. Lett. **99**, 150405 (2007); V. Krachmalnicoff *et al.*, *ibid.* **104**, 150402 (2010); P. Ziń, J. Chwedenczuk, A. Veitia, K. Rzazewski, and M. Trippenbach, *ibid.* **94**, 200401 (2005); P. Ziń, J. Chwedeńczuk, and M. Trippenbach, Phys. Rev. A **73**, 033602 (2006); J. Chwedeńczuk, P. Ziń, M. Trippenbach, A. Perrin, V. Leung, D. Boiron, and C. I. Westbrook, *ibid.* **78**, 053605 (2008); Wu RuGway, S. S. Hodgman, R. G. Dall, M. T. Johnsson, and A. G. Truscott, Phys. Rev. Lett. **107**, 075301 (2011).
[11] W. Vassen *et al.*, Rev. Mod. Phys. **84**, 175 (2012).
[12] M.-O. Mewes, M. R. Andrews, D. M. Kurn, D. S. Durfee, C. G. Townsend, and W. Ketterle, Phys. Rev. Lett. **78**, 582 (1997);

D. S. Durfee and W. Ketterle, Opt. Express **2**, 299 (1998); B. P. Anderson and M. A. Kasevich, Science **282**, 1686 (1998); E. W. Hagley *et al*., *ibid*. **283**, 1706 (1999); I. Bloch, T. W. Hänsch, and T. Esslinger, Phys. Rev. Lett. **82**, 3008 (1999); Y. Le Coq, J. H. Thywissen, S. A. Rangwala, F. Gerbier, S. Richard, G. Delannoy, P. Bouyer, and A. Aspect, *ibid*. **87**, 170403 (2001).

[13] A. D. Cronin, J. Schmiedmayer, and D. E. Pritchard, Rev. Mod. Phys. **81**, 1051 (2009).

[14] V. V. Konotop, Phys. Rev. E **54**, 4266 (1996).

[15] K. M. Hilligsøe and K. Mølmer, Phys. Rev. A **71**, 041602 (2005); N. Gemelke, E. Sarajlic, Y. Bidel, S. Hong, and S. Chu, Phys. Rev. Lett. **95**, 170404 (2005).

[16] G. K. Campbell, J. Mun, M. Boyd, E. W. Streed, W. Ketterle, and D. E. Pritchard, Phys. Rev. Lett. **96**, 020406 (2006).

[17] V. Berger, Phys. Rev. Lett. **81**, 4136 (1998).

[18] R. Yamazaki, S. Taie, S. Sugawa, and Y. Takahashi, Phys. Rev. Lett. **105**, 050405 (2010).

[19] A. V. Yulin, Yu. V. Bludov, V. V. Konotop, V. Kuzmiak, and M. Salerno, Phys. Rev. A **84**, 063638 (2011); **87**, 033625 (2013).

[20] L. Salasnich and B. A. Malomed, J. Phys. B **45**, 055302 (2012).

[21] T. Wasak, V. V. Konotop, and M. Trippenbach, in press (2013).

[22] V. A. Brazhnyi and V. V. Konotop, Phys. Rev. A **68**, 043613 (2003).